

Signature of smooth transition from diabatic to adiabatic states in heavy-ion fusion reactions at deep subbarrier energies

Takatoshi Ichikawa,¹ Kouichi Hagino,² and Akira Iwamoto³

¹*Yukawa Institute for Theoretical Physics, Kyoto University, Kyoto 606-8502, Japan*

²*Department of Physics, Tohoku University, Sendai 980-8578, Japan*

³*Japan Atomic Energy Agency, Tokai-mura, Naka-gun, Ibaraki 319-1195, Japan*

(Dated: July 25, 2018)

We propose a novel extension of the standard coupled-channels framework for heavy-ion reactions in order to analyze fusion reactions at deep subbarrier incident energies. This extension simulates a smooth transition between the diabatic two-body and the adiabatic one-body states. To this end, we damp gradually the off-diagonal part of the coupling potential, for which the position of the onset of the damping varies for each eigen channel. We show that this model accounts well for the steep falloff of the fusion cross sections for the $^{16}\text{O}+^{208}\text{Pb}$, $^{64}\text{Ni}+^{64}\text{Ni}$, and $^{58}\text{Ni}+^{58}\text{Ni}$ reactions.

PACS numbers: 25.60.Pj, 24.10.Eq, 25.70.Jj, 25.70.-z

Heavy-ion fusion reactions at low incident energies provide a good opportunity to study fundamental features of the tunneling phenomena in many-particle systems. A potential barrier, called the Coulomb barrier, is formed because of a strong cancellation between the repulsive Coulomb interaction and an attractive nuclear interaction. In particular, the potential tunneling at incident energies below the Coulomb barrier is referred to as the subbarrier fusion reaction. One prominent feature of the subbarrier fusion reactions is the large enhancement of fusion cross sections, as compared to a prediction of the simple potential tunneling [1]. This enhancement has been attributed to the coupling of the relative motion between the colliding nuclei to several intrinsic degrees of freedom, such as a collective vibration of the target and/or projectile nuclei. The coupled-channels (CC) approach, based on this picture, has been successful in accounting for the subbarrier enhancement [2].

Because of a recent progress in experimental techniques, it has been possible to measure fusion cross sections down to deep-subbarrier incident energies [3, 4, 5, 6]. These data show a substantial reduction of fusion cross sections at deep-subbarrier energies from the prediction of the CC calculations that reproduce the experimental data at energies around the Coulomb barrier, and have brought about a renewed interest in this field. This phenomenon, often referred to as the fusion hindrance, shows a threshold behavior, where the data deviate largely from the standard CC calculations at incident energies below a certain threshold energy, E_s .

A key element to understand the fusion hindrance is the density overlap of the colliding nuclei in the potential tunneling process. When the incident energy is below the potential energy at the touching point of the colliding nuclei, V_{Touch} , the inner turning point of the potential is located inside the touching point, and the projectile is still in the classically forbidden region when the two nuclei touch with each other (see Fig.1 in Ref.[7]). In this situation, the colliding nuclei have to penetrate through a residual barrier with an overlapping configuration before fusion takes place. In our previous work [7], we evaluated V_{Touch} using several kinds of ion-ion potential, and systematically compared those with experimentally de-

termined threshold energy E_s for many systems. The obtained systematics shows a strong correlation between V_{Touch} and E_s , indicating strongly that the nuclear interaction in the overlapping region plays a decisive role in the deep-subbarrier hindrance.

Three different mechanisms have been proposed so far in order to account for the fusion hindrance. Based on the sudden picture, Mişcu and Esbensen have investigated the effect of the nuclear interaction in the overlap region, in terms of a repulsive core due to the Pauli exclusion principle [8, 9, 10]. Assuming the frozen-density in the overlapping region, they obtained a much shallower potential pocket than the standard one, which hinders the fusion probability for high partial waves. Their shallow potential reproduces well the fusion hindrance. In contrast, we have proposed the adiabatic approach by assuming neck formations between the colliding nuclei in the overlap region [11]. In our model, the fusion hindrance originates from the tunneling of much thicker potential barrier characterized by the adiabatic one-body potential. This model achieved comparable good reproduction of the experimental data to the sudden model. The third mechanism, suggested recently by Dasgupta *et al.*, is the quantum decoherence of channel wave functions caused by the coupling to the thermal bath [5]. A model calculation based on this picture shows a possibility of the gradual occurrence of hindrance in subbarrier fusion reactions [12].

Among those three mechanisms, the origin for the deep-subbarrier hindrance is considerably different from each other. The recent precise data for the $^{16}\text{O}+^{208}\text{Pb}$ fusion [5] may provide an adequate system to discriminate among the various models, because the behavior of its astrophysical S-factor is difficult to reproduce within a simple model calculation. In the model of Esbensen and Mişcu, not only the collective inelastic channels but also the particle transfer channel with modified coupling strengths are necessary for a fit to the experimental data [8]. In the estimation of Dasgupta *et al.*, it was impossible to obtain an overall fit to the experimental data from the above-barrier to deep-subbarrier regions with a single parameter set for the nuclear potential [5]. On the other hand, the performance of the adiabatic model has not yet been studied

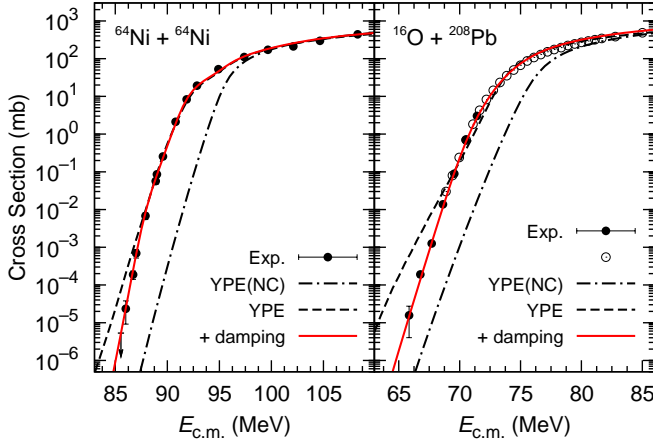


FIG. 1: (Color online) Fusion cross sections for the $^{64}\text{Ni}+^{64}\text{Ni}$ and $^{16}\text{O}+^{208}\text{Pb}$ systems. The solid and the dashed lines are the calculated result with and without the damping factor, respectively. The dot-dashed line is the result of no coupling with the YPE potential.

for this system, although the concept of the adiabatic potential was proved helpful in the analysis of the potential inversion method in the deep-subbarrier fusion [13].

In this paper, we attempt to study the deep-subbarrier fusion for the $^{16}\text{O}+^{208}\text{Pb}$ reaction based on the adiabatic model. Our previous model has a defect that the full quantum treatment for the two-body part suddenly switches to the semi-classical one for the adiabatic one-body part, which introduces arbitrariness for the choice of the Hamiltonian. To avoid the shortcoming, we develop below a full quantum mechanics where the CC approach in the two-body system are smoothly jointed to the adiabatic potential tunneling for the one-body system, resulting in an overall good agreement for the $^{16}\text{O}+^{208}\text{Pb}$ reaction, as well as for the $^{58}\text{Ni}+^{58}\text{Ni}$ and $^{64}\text{Ni}+^{64}\text{Ni}$ systems.

We employ the incoming wave boundary condition in order to simulate a compound nucleus formation. In order to construct an adiabatic potential model with it, we postulate the followings: (1) Before the target and projectile nuclei touch with each other, the standard CC model in the two-body system works well. (2) After the target and projectile overlap appreciably with each other, the fusion process is governed by a single adiabatic one-body potential where the excitation on the adiabatic base is neglected. (3) The transition from the two-body treatment to the one-body one takes place at near the touching configuration, where all physical quantities are smoothly joined.

To this end, we adopt Yukawa-plus-exponential (YPE) potential [14] as a basic ion-ion potential $V_N^{(0)}$, because the diagonal part of this potential satisfies the conditions (1)-(3) by choosing a suitable neck-formed shape for the one-body system, as has been shown in our previous work [11]. In addition, the saturation property of the nuclear matter is phenomenologically taken into account in the YPE model. It has also been shown that the YPE model is consistent with the potential obtained with the energy density formalism with the Skyrme SkM* interaction [15, 16].

The nuclear coupling form factor which describes excita-

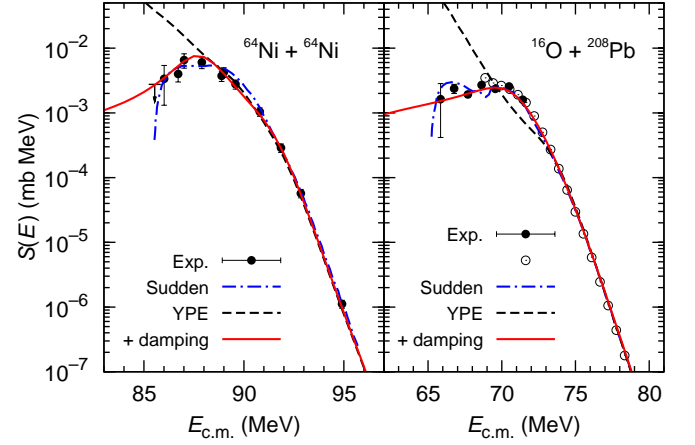


FIG. 2: (Color online) Astrophysical S-factor for the $^{64}\text{Ni}+^{64}\text{Ni}$ and $^{16}\text{O}+^{208}\text{Pb}$ systems as a function of the incident energies. The meaning of each line is the same as in Fig. 1 except for the dot-dashed line, which shows the result of the sudden model taken from Refs. [10] and [8].

tions to the vibrational states in the two-body channel is taken as the derivative of potential $V_N^{(0)}$ [17]. The coupling matrix elements are evaluated with the eigen-channel representation as in Eq. (24) in Ref.[18]. In order to satisfy the conditions (1)-(3), we employ the following form for the nuclear potential for the eigen-channel α ,

$$V_N(r, \lambda_\alpha) = V_N^{(0)}(r) + \left[-\frac{dV_N^{(0)}}{dr} \lambda_\alpha + \frac{1}{2} \frac{d^2 V_N^{(0)}}{dr^2} \lambda_\alpha^2 \right] \Phi(r, \lambda_\alpha), \quad (1)$$

where λ_α is the eigen value of the excitation operator. The most important modification from the standard CC treatment is the introduction of the damping factor Φ . This damping factor represents the physical process for the gradual transition to the adiabatic approximation, by diminishing the strength of excitations to the target and/or projectile vibrational states after the two nuclei overlap with each other. We thus choose the damping factor given by

$$\Phi(r, \lambda_\alpha) = \begin{cases} 1 & r \geq R_d + \lambda_\alpha \text{ (Two-body region),} \\ e^{-\frac{(r-R_d-\lambda_\alpha)^2}{2a_d^2}} & r < R_d + \lambda_\alpha \text{ (Overlap region),} \end{cases} \quad (2)$$

where R_d is the spherical touching distance between the target and projectile defined by $R_d = r_d(A_T^{1/3} + A_P^{1/3})$, r_d is the damping radius parameter, and a_d is the damping diffuseness parameter. Notice that the touching point in the damping factor depends on λ_α , that is, the strength of the excitations starts to decrease at the different distance in each eigen channel.

It is slightly complicated to take into account the effect of the damping factor on the Coulomb coupling. When different multipole components are present simultaneously, the eigen channels, which are introduced to evaluate the nuclear coupling matrix elements, do not diagonalize the Coulomb coupling matrix. We have therefore introduced the channel independent damping factor for the Coulomb coupling, but the

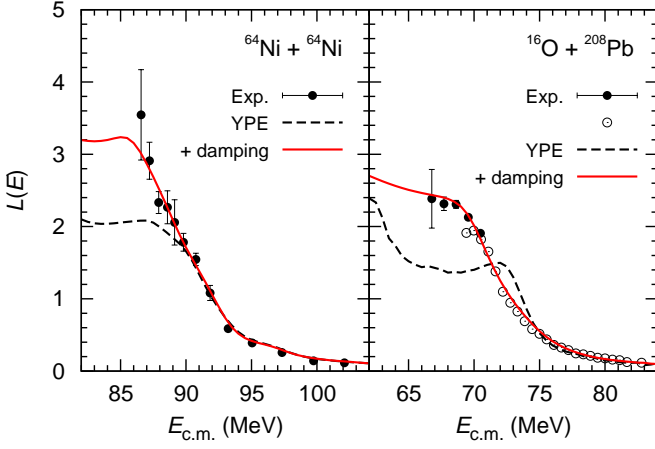


FIG. 3: (Color online) Logarithmic derivatives of fusion cross sections, $L(E) = d \ln(E_{c.m.} \sigma_{fus}) / d E_{c.m.}$, for the $^{64}\text{Ni} + ^{64}\text{Ni}$ and $^{16}\text{O} + ^{208}\text{Pb}$ systems as a function of the incident energies. The meaning of each line is the same as in Fig. 1.

effect on the fusion cross sections appeared small. For simplicity, we therefore consider the damping factor only for the nuclear coupling in the calculations presented below.

We apply our present model to the fusion reactions for the $^{64}\text{Ni} + ^{64}\text{Ni}$ and $^{16}\text{O} + ^{208}\text{Pb}$ systems. To this end, we incorporate the damping factor and the YPE potential in the computer code *ccfull* [18]. For the $^{64}\text{Ni} + ^{64}\text{Ni}$ system, the coupling scheme included in the calculation, as well as the deformation parameters, are the same as in Ref. [4]. For the $^{16}\text{O} + ^{208}\text{Pb}$ system, those are the same as in Ref. [19], but we include the coupling to the low-lying 3^- phonon states and the double-octupole phonon excitations for both the ^{16}O and ^{208}Pb nuclei. For the damping factor, we use $r_d = 1.298$ fm and $a_d = 1.05$ fm for the $^{64}\text{Ni} + ^{64}\text{Ni}$ system, and $r_d = 1.280$ fm and $a_d = 1.28$ fm for the $^{16}\text{O} + ^{208}\text{Pb}$ system.

For the YPE model, the parameters are taken as $a_0 = 0.68$ fm, $a_s = 21.33$ MeV, and $\kappa_s = 2.378$ from FRLDM2002 [20]. In order to fit the experimental fusion cross sections, the radius parameter r_0 is adjusted to be 1.205 fm and 1.202 fm for the $^{64}\text{Ni} + ^{64}\text{Ni}$ and $^{16}\text{O} + ^{208}\text{Pb}$ systems, respectively. For the mass asymmetric $^{16}\text{O} + ^{208}\text{Pb}$ system, it is difficult to joint smoothly the potential energies between the two-body and the adiabatic one-body systems at the touching point, because the proton-to-neutron ratio for the one-body system differs from that for the target and projectile in the two-body system. To avoid this difficulty, we smoothly connect the potential energy around the touching point to the liquid-drop energy of the compound nucleus, using the third-order polynomial function (see. the dashed line in Fig. 4). We do this by identifying the internucleus distance r with the centers-of-masses distance of two half spheres. The obtained potential is similar to the result of the density-constrained time-dependent Hartree-Fock method [21]. We have checked this prescription for the mass symmetric $^{64}\text{Ni} + ^{64}\text{Ni}$ system, by comparing to the potential energy used in our previous work [11]. The deviation due to this prescription is negligibly small.

Figure 1 shows the fusion cross sections thus obtained. The

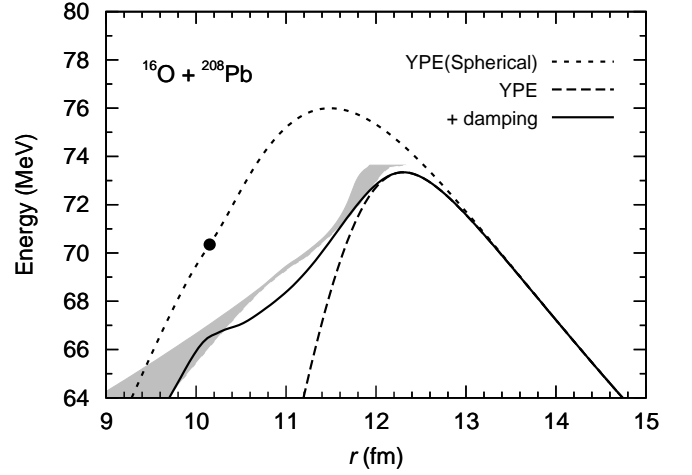


FIG. 4: The adiabatic potential for the $^{16}\text{O} + ^{208}\text{Pb}$ system as a function of the center-of-mass distance. The solid line is the adiabatic potential obtained with the damping factor. The dashed line is the result obtained with the conventional CC approach. The dotted line and the solid circle are the potential and the touching point for the uncoupled case, respectively. The gray region denotes the adiabatic potential obtained with the potential inversion method, taken from Ref. [13].

fusion cross sections obtained with the damping factor are in good agreement with the experimental data for both the systems (see the solid line). The dashed line is the YPE potentials without the damping factor. The dot-dashed line is the results of no coupling with the YPE potential. For both the systems, we see that drastic improvement has been achieved by taking into account the damping of the CC form factors.

We also compare the astrophysical S factor representation of the experimental data with the calculated results, as shown in Fig. 2. In the calculation, the Sommerfeld parameter η is shifted by 75.23 and 49.0 for the $^{64}\text{Ni} + ^{64}\text{Ni}$ and $^{16}\text{O} + ^{208}\text{Pb}$ systems, respectively. The S factor obtained with the damping factor are consistent with the experimental data for both the systems (see the solid lines), and reproduce well the peak structure.

For astrophysical interests, it is important to evaluate fusion cross sections at extremely low incident energies, which is difficult to measure directly. Notice that the S factor predicted by our model differs considerably from that of the sudden model by Mişcu and Esbensen [10], denoted by the dot-dashed line. For both the systems, as the incident energy decreases, their S factor falls off steeply below the peak of the S factor, while our S factor has a much weaker energy dependence.

Figure 3 compares the logarithmic derivatives $d \ln(E_{c.m.} \sigma_{fus}) / d E_{c.m.}$ of the experimental fusion cross section with the calculated results. It is again remarkable that only the result with the damping factor achieves nice reproduction of the experimental data. For the $^{64}\text{Ni} + ^{64}\text{Ni}$ system, the result with the damping factor becomes saturated below $E_{c.m.} = 86$ MeV. This behavior is similar to the experimental data for the $^{16}\text{O} + ^{208}\text{Pb}$ system. The measurement at further lower incident energies for this system will thus provide a

strong test for the present adiabatic model.

Figure 4 shows the adiabatic potential of the $^{16}\text{O}+^{208}\text{Pb}$ system, that is, the lowest eigenvalue obtained by diagonalizing the coupling matrix at each center-of-mass distance r . The adiabatic potential calculated with and without the damping factor are denoted by the solid and the dashed lines, respectively. The uncoupled YPE potential is also shown by the dotted line. The solid circle denotes the touching point in the absence of channel coupling. We see that the result obtained with the damping factor is much thicker than that of the conventional CC model. In this respect, it is interesting that the result with the damping factor is similar to that obtained with the potential inversion method [13], denoted by the gray region, justifying our treatment for the damping of the CC form factor.

For the average angular momentum of the compound nucleus, the results with the damping factor become saturated at incident energies below the threshold energy with decreasing incident energy, as shown in our previous works [11, 22]. This result largely differs from that obtained with the sudden model by Mişcu and Esbensen. Their result is strongly suppressed at energies below the threshold energy. It is thus interesting to measure the average angular momentum at deep subbarrier energies, in order to discriminate the two approaches.

We have also applied our model to the $^{58}\text{Ni}+^{58}\text{Ni}$ reactions and the results obtained are in good agreement with the experimental data. For the damping factor, we used $r_d = 1.3$ fm and $a_d = 1.3$ fm in order to fit the experimental data. Notice that

the obtained damping radius parameters for the three systems which we study are almost the same. We emphasize that our model achieves an overall fit not only to the fusion cross sections but also to the S factors and the logarithmic derivatives simultaneously.

In summary, we have proposed a novel coupled-channels approach for heavy-ion fusion reactions by introducing the damping of the CC form factor inside the touch point in order to simulate the transition from the diabatic to adiabatic states. The important point in our present model is that the transition takes place at different places for each eigen channel. By applying this model to the $^{16}\text{O}+^{208}\text{Pb}$, the $^{64}\text{Ni}+^{64}\text{Ni}$, and the $^{58}\text{Ni}+^{58}\text{Ni}$ systems, we conclude that the smooth transition from the diabatic two-body to the adiabatic one-body potential is responsible for the steep falloff of the fusion cross section. It is an interesting future study to apply the present model systematically to other systems and clarify the dynamics of deep subbarrier fusion reactions, and thus many-particle tunneling phenomena.

Acknowledgments

T.I. thanks H. Feldmeier for useful discussions. This work was supported by the Japanese Ministry of Education, Culture, Sports, Science and Technology by Grant-in-Aid for Scientific Research under the program number 19740115.

-
- [1] M. Dasgupta, D. J. Hinde, N. Rowley, and A. M. Stefanini, *Annu. Rev. Nucl. Part. Sci.* **48**, 401 (1998).
 - [2] A. B. Balantekin and N. Takigawa, *Rev. Mod. Phys.* **70**, 77 (1998).
 - [3] C.L. Jiang *et al.*, *Phys. Rev. Lett.* **89**, 052701 (2002); *Phys. Rev. C* **69**, 014604 (2004); *Phys. Rev. C* **71**, 044613 (2005); *Phys. Rev. C* **73**, 014613 (2006); *Phys. Rev. C* **75**, 057604 (2007); *Phys. Rev. C* **78**, 017601 (2008); *Phys. Rev. C* **79**, 044601 (2009).
 - [4] C. L. Jiang, K. E. Rehm, R. V. F. Janssens, H. Esbensen, I. Ahmad, B. B. Back, P. Collon, C. N. Davids, J. P. Greene, D. J. Henderson, *et al.*, *Phys. Rev. Lett.* **93**, 012701 (2004);
 - [5] M. Dasgupta, D. J. Hinde, A. Diaz-Torres, B. Bouriquet, C. I. Low, G. J. Milburn, and J. O. Newton, *Phys. Rev. Lett.* **99**, 192701 (2007).
 - [6] A.M. Stefanini *et al.*, *Phys. Rev. C* **78**, 044607 (2008); *Phys. Lett. B* **679**, 95 (2009).
 - [7] T. Ichikawa, K. Hagino, and A. Iwamoto, *Phys. Rev. C* **75**, 064612 (2007).
 - [8] H. Esbensen and Ş. Mişcu, *Phys. Rev. C* **76**, 054609 (2007).
 - [9] Ş. Mişcu and H. Esbensen, *Phys. Rev. Lett.* **96**, 112701 (2006).
 - [10] Ş. Mişcu and H. Esbensen, *Phys. Rev. C* **75**, 034606 (2007).
 - [11] T. Ichikawa, K. Hagino, and A. Iwamoto, *Phys. Rev. C* **75**, 057603 (2007).
 - [12] A. Diaz-Torres, D. J. Hinde, M. Dasgupta, G. J. Milburn, and J. A. Tostevin, *Phys. Rev. C* **78**, 064604 (2008).
 - [13] K. Hagino and Y. Watanabe, *Phys. Rev. C* **76**, 021601(R) (2007).
 - [14] H. J. Krappe, J. R. Nix, and A. J. Sierk, *Phys. Rev. C* **20**, 992 (1979).
 - [15] L. C. Vaz, J. M. Alexander, and G. R. Satchler, *Phys. Rep.* **69**, 373 (1981).
 - [16] V. Yu. Denisov and W. Nörenberg, *Eur. Phys. J. A* **15**, 375 (2002).
 - [17] H. Esbensen and S. Landowne, *Phys. Rev. C* **35**, 2090 (1987).
 - [18] K. Hagino, N. Rowley, and A. T. Kruppa, *Comput. Phys. Commun.* **123**, 143 (1999).
 - [19] C. R. Morton, A. C. Berriman, M. Dasgupta, D. J. Hinde, J. O. Newton, K. Hagino, and I. J. Thompson, *Phys. Rev. C* **60**, 044608 (1999).
 - [20] P. Möller, A. J. Sierk, and A. Iwamoto, *Phys. Rev. Lett.* **92**, 072501 (2004).
 - [21] A. S. Umar and V. E. Oberacker, *Phys. Rev. C* **77**, 064605 (2008); *Eur. Phys. J. A* **39**, 243 (2009).
 - [22] T. Ichikawa, K. Hagino, and A. Iwamoto, *AIP Conf. Proc.* **1098**, 32 (2009).